

Effects of two-particle–two-hole configurations and tensor force on β decay of magic nuclei

M. J. Yang,¹ H. Sagawa,^{2,3} C. L. Bai¹, and H. Q. Zhang⁴¹College of Physics, Sichuan University, Chendu 610065, China²Center for Mathematics and Physics, University of Aizu, Aizu-Wakamatsu, Fukushima 965-8560, Japan³RIKEN, Nishina Center, Wako 351-0198, Japan⁴China Institute of Atomic Energy, Beijing 102413, China

(Received 26 October 2022; revised 18 December 2022; accepted 6 January 2023; published 30 January 2023)

The β -decay half-lives of four semimagic and magic nuclei, ^{34}Si , $^{68,78}\text{Ni}$, and ^{132}Sn , have been investigated using the self-consistent Hartree-Fock (HF) plus subtracted second random-phase approximation (SSRPA) model with Skyrme energy density functions (EDFs). The inclusion of the two-particle–two-hole (2p-2h) configurations in SSRPA model shifts low-lying Gamow-Teller (GT) states downward. It leads to an increase of the β -decay phase space, which ensures the half-lives of the four nuclei are finite and reduces the β -decay half-lives dramatically. The effect of tensor interaction on the β -decay half-life in the SSRPA model is to change the half-lives greatly by about one to two orders of magnitude with respect to the ones obtained without tensor force.

DOI: [10.1103/PhysRevC.107.014325](https://doi.org/10.1103/PhysRevC.107.014325)

I. INTRODUCTION

Nuclear β decay is a weak interaction process which plays a significant role in the neutron capture process of stellar nucleosynthesis [1,2]. The β -decay rates set the timescale of the rapid neutron capture process (r-process), which is responsible for the synthesis of half of the nuclei heavier than iron and all heavy actinide nuclei [3–7].

With the development of radioactive ion-beam facilities, important advances and improvements in the measurements of nuclear β -decay half-lives have been achieved in recent years [8–10] (more experimental data can be found in Refs. [11–13]). However, many nuclei of interest in the astrophysical processes are far from stability, and the β -decay properties of these nuclei are available mostly by theoretical evaluations. Various theoretical models have been developed for this purpose, for example, the macroscopic gross theory, which adopts the sum rule of the β -decay strength function, as well as the final level density can estimate the β -decay half-lives for the entire nuclide chart [14–16]. Microscopically, two models have been widely used in the calculations of nuclear β -decay half-lives: the shell model [17,18] and the proton-neutron (pn) quasiparticle random-phase approximation (QRPA) [19,20].

The nuclear shell-model reproduces reasonably the experimental β -decay half-lives of the waiting-point nuclei at $N = 50, 82, 126$ [21–28]. However, the shell model studies are limited to light to medium-heavy nuclei or those near the closed shells because of their huge configuration space. The pn-QRPA model can be applied in general to calculate the β decays of all nuclei in the whole nuclide chart [29–37]. In the (Q)RPA approach, however, low-lying 1^+ Gamow-Teller (GT) states of daughter nuclei are often predicted at rather

higher energy, and consequently the estimated half-lives become longer than the experimental data. This deficiency can be cured to a certain extent in the case of open-shell nuclei by the inclusion of an attractive isoscalar pairing force [29–31]. However, the isoscalar pairing has a negligible effect on magic or semimagic nuclei such as ^{78}Ni and ^{132}Sn and does not help to improve the predictions of half-lives of closed-shell nuclei.

The deficiency of the previous (Q)RPA results on the magic and semimagic nuclei indicates that there must exist other correlations than the isoscalar pairing. To reduce the half-lives of semimagic and/or magic nuclei, one promising candidate is the tensor force. As an important ingredient of nuclear force, the tensor force was reported to play a significant role in the evaluation of β -decay rates [38–41]. Another important strategy is the inclusion of higher correlations beyond the RPA or QRPA calculations. In particular, the RPA is restricted to one-particle–one-hole (1p-1h) configuration space and this configuration is known as being not sufficient for the description of the spreading width of the giant resonances [42,43]. To accommodate configuration space higher than 1p-1h excitations, the phonon-phonon coupling model [44] and the RPA+particle-vibrations coupling (PVC) model [45] have been applied to the β decays. The RPA+PVC model was later extended to the quasiparticle vibration coupling (QVC) plus QRPA model and then applied to the study of β decays in the open-shell nuclei [46,47]. These works achieve much improvement on β decay half-life evaluations with the Skyrme EDF SkM*.

Recently, subtracted second random-phase approximation (SSRPA) model, which fully include the 1p-1h and 2p-2h configurations, was applied to the study of GT states in several magic and semimagic nuclei in Refs. [48,49]. In these works, large quenching factors close to the experimental ones for

the GT sum rules were obtained, and the predicted β -decay half-life agrees better with the experiment value than the other beyond-mean-field models due to the explicit inclusion of 2p-2h configurations. Very recently, the tensor force was included in the SSRPA calculations of four magic nuclei ^{48}Ca , ^{90}Zr , ^{132}Sn , and ^{208}Pb [50]. It was found that the tensor force is important to reproduce systematically the excitation energies and strengths of the giant GT resonances, and also shifts about 10% of the total GT strength to the high-energy region of more than 25 MeV.

Since both the tensor force and the 2p-2h correlations are expected to have significant effects on the half-lives of β decay in magic and semimagic nuclei, we apply the SSRPA model including tensor force to the β -decay half-lives in magic and semimagic nuclei, ^{34}Si , $^{68,78}\text{Ni}$, and ^{132}Sn with Skyrme EDFs. The article is organized as follows. In Sec. II, a short description of the formalism and some numerical details are presented. In Sec. III, the effects of 2p-2h configurations and tensor force on the half-lives of β decay are discussed quantitatively. A summary is given in Sec. IV.

II. THEORETICAL MODELS AND NUMERICAL DETAILS

As the SRPA and SSRPA models are well described in many works [51–54], we sketch briefly the formulas about β decay and also about our numerical details. The β decay of nuclei presently studied is dominated by the GT transition with the operator

$$\hat{O}_{\text{GT}}^{\pm} = \sum_{i=1}^A \sigma(i)t_{\pm}(i), \quad (1)$$

where σ is the spin operator and $t_{\pm} = t_x \pm it_y$ are the isospin raising and lowering operators, respectively. In principle, the t_- channel and t_+ channel are correlated in RPA or SSRPA, but in the nuclei with large enough neutron excess, the t_+ channel is strongly blocked and may have only negligible contributions for the t_- channel. We did SSRPA and subtracted second Tamm-Dancoff approximation (SSTDA) calculations with and without the t_+ channel, respectively, and found that there are invisible differences between two calculations.

The corresponding GT strength is defined as

$$B_{1_n^+}^{\text{GT}^{\pm}} = |\langle 1_n^+ | \hat{O}_{\text{GT}}^{\pm} | 0 \rangle|^2, \quad (2)$$

where $|1_n^+\rangle$ is the n th $J^{\pi} = 1^+$ state. Once the GT states have been obtained from the HF+SSRPA calculations, the GT-type β -decay half-life can be calculated using the formula [29]

$$T_{1/2} = \frac{D}{g_A^2 \sum_n B_{1_n^+}^{\text{GT}^-} f_0(Z, A, \omega_n)}, \quad (3)$$

where $D = 6163.4 \pm 3.8$ s (e.g., see Ref. [55]), $f_0(Z, A, \omega_n)$ is the integrated phase factor, ω_n is the excitation energy of n th GT state calculated with reference to the ground state of mother nucleus, and $g_A \equiv G_A/G_V = 1.26$ is the ratio of the axial-vector and vector coupling constants. The value g_A is usually set to lower than 1.26 assuming a quenching factor which is closely related to the GT sum rule deficiency [17]. In this work, the value g_A is set to be $g_A = 1.0$. This value is consistent with the quenching factor in our previous work

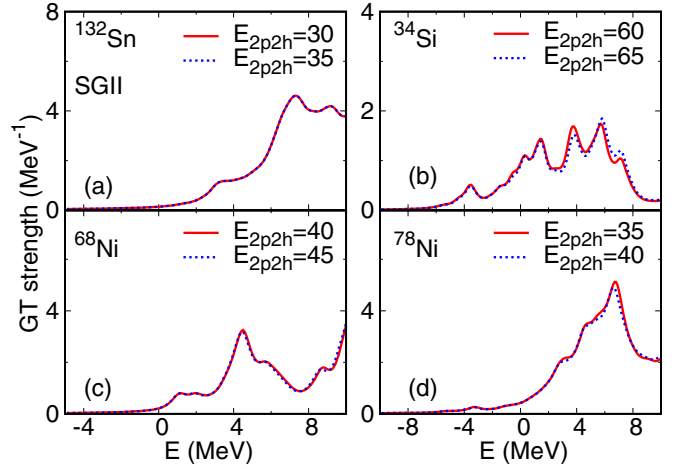


FIG. 1. The GT strength distributions at the energy region lower than 10 MeV calculated by SSRPA with SGII in ^{132}Sn , ^{68}Ni , ^{34}Si , and ^{78}Ni . The red solid lines represent results with the cutoff adopted in the article. The blue dashed lines represent results with 5 MeV higher cutoff energy than the red ones. The calculated discrete strength distributions are smoothed by a Lorentzian weighting function of 1 MeV width.

on the study of GT transition strengths by SSRPA model [50]. The sum about n runs over all 1^+ states within the β -decay energy window $Q = \Delta_{nH} - \omega_n > 0$ MeV, with $\Delta_{nH} = 0.78227$ MeV denoting the mass difference between the neutron and hydrogen atom. When the energy is referred to the ground state of the daughter nucleus, the excitation energy is defined as $E_n = \omega_n - \Delta B$, where $\Delta B = B(Z, N) - B(Z + 1, N - 1)$ is the experimental binding energy difference of mother and daughter nuclei. This choice is convenient, because the calculated energy of the final 1^+ states can be directly compared to the experimental spectrum of the final nucleus (such as Fig. 5). Then the upper limit of integration in Eq. (3) becomes equal to the value $Q_\beta = \Delta_{nH} - \Delta B$, which is the experimental energy of β decay. When all the GT states are above the Q_β window, the nucleus is stable.

In the present SSRPA calculations for GT states, we perform full calculations for both 1p-1h and 2p-2h configuration space of all nuclei except ^{132}Sn . We adopt for ^{132}Sn the diagonal approximation of A_{22} in the subtraction matrices of A_{11} sector, while the full calculations are performed otherwise even in ^{132}Sn . We checked that the adoption of a diagonal approximation of A_{22} in the subtraction procedure for ^{132}Sn does not change any important information in the excitation spectrum [49,50]. In calculating A_{22} , all the matrices including the 4-particle or 4-hole states (Eq. (7) of [54]) are included in our calculations. For the 1p-1h configuration space, the energy cutoff is set as 100 MeV, while for the 2p-2h configurations, the cutoffs are set as 60 MeV for ^{34}Si , 40 MeV for ^{68}Ni , 35 MeV for ^{78}Ni , and 30 MeV for ^{132}Sn . Figure 1 shows the convergence of GT strength distributions at the low-energy region below 10 MeV by different cutoff energies for 2p-2h configurations. These results indicate that the calculated GT strengths are rather stable for the energy cutoff and the β -decay lifetimes may not change appreciably even when the

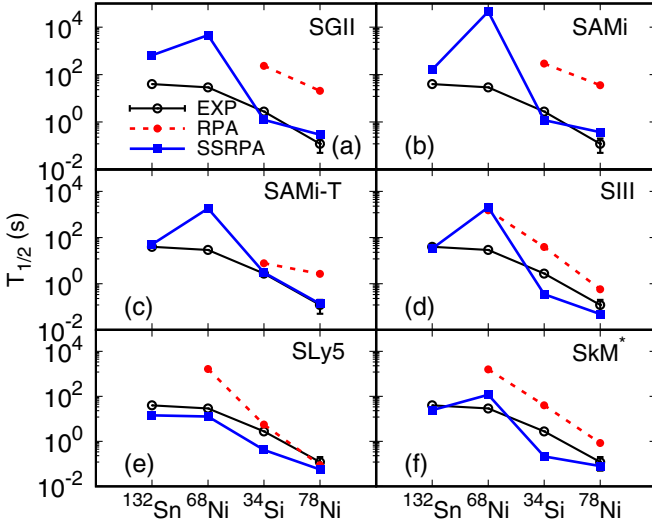


FIG. 2. The β -decay half-lives of ^{132}Sn , ^{68}Ni , ^{34}Si , and ^{78}Ni calculated by RPA and SSRPA models, respectively, in comparisons with experimental values [13]. The red solid circles and the blue solid squares represent results obtained by RPA and SSRPA respectively. The experimental data are shown by the black empty circles. The RPA results are infinite in some nuclei and not shown in the figure.

cutoff is raised beyond these limits. Because of these good convergence features, we adopt the lower energy cutoffs in Fig. 1 for the following calculations. In this work, Skyrme EDFs SkM* [56], SIII [57], SLy5 [58], SGII [59], SAMi [60], and SAMi-T [61] are employed.

III. RESULTS AND DISCUSSION

In this section, we study first the effect of the 2p-2h correlations taken into account in the SSRPA model on the β -decay half-lives of the four semimagic and magic nuclei ^{132}Sn , ^{68}Ni , ^{34}Si , and ^{78}Ni . Figure 2 shows the β -decay half-lives calculated by RPA and SSRPA models, in comparison with experimental values. The RPA results largely overestimate the half-lives for almost all nuclei. Nuclei are sometimes stable in RPA calculations such as ^{132}Sn , and the half-lives are infinite and not shown in this figure. On the other hand, the half-lives of all nuclei calculated with SSRPA become finite values and become close to the experimental values. In the case of ^{68}Ni , we can see some discrepancies between the results of SSRPA and the experiments. In Fig. 2, the SSRPA results of EDFs SLy5 and SkM* give better agreements of the half-lives in the four nuclei than the other EDFs in comparisons with the experimental data. Similar results were obtained by RPA+PVC calculations [45].

In our previous SSRPA calculations [50], we found that SGII, SAMi, and SAMi-T EDFs can systematically well reproduce the giant GT strength distributions in four magic nuclei ^{48}Ca , ^{90}Zr , ^{132}Sn , and ^{208}Pb . On the other hand, SLy5 and SkM* give rather poor results for the giant GT states. As shown in Figs. 2(a) and 2(b), the calculated half-lives in ^{34}Si and ^{78}Ni are reduced about by two order of magnitude in SSRPA calculations with the SGII and SAMi, and reproduce well the experimental results. In Fig. 2(c), the tensor force is

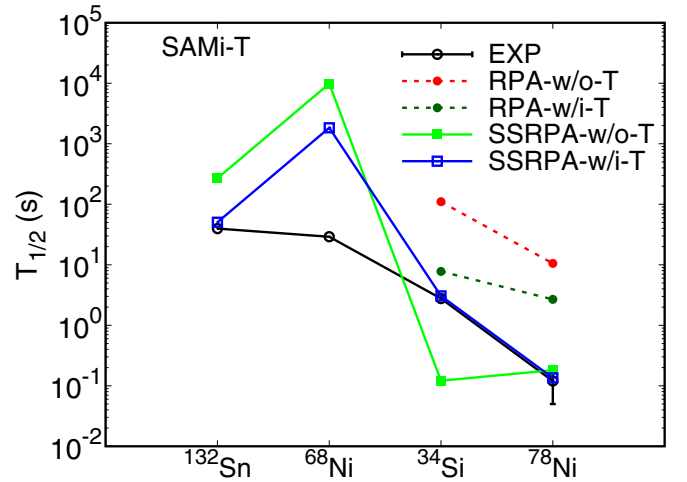


FIG. 3. The β -decay half-lives of ^{132}Sn , ^{68}Ni , ^{34}Si , and ^{78}Ni calculated by RPA and SSRPA with SAMi-T including or excluding tensor terms in comparison with the experimental values [13]. The red and dark green solid circles represent results obtained by RPA with SAMi-T excluding and including tensor terms respectively, labeled by “RPA-w/o-T” and “RPA-w/i-T.” The green squares are SSRPA results with SAMi-T without tensor terms labeled by “SSRPA-w/o-T.” The blue empty squares show SSRPA results with SAMi-T with tensor terms labeled “SSRPA-w/i-T.” The experimental data are shown by the black empty dot.

included in SAMi-T EDF, and the inclusion of tensor force can dramatically reduce the half-lives in RPA calculation compared with SAMi in Fig. 2(b) without the tensor terms in EDFs. In addition, comparing the results obtained with SAMi and SAMi-T in SSRPA calculations, the tensor interaction obviously reduces the half-lives of ^{132}Sn and ^{68}Ni , by factors of about 4 and 25, respectively.

While the parameter sets of SAMi and SAMi-T are optimized for the same data set, the central part of EDF is slightly different from each other due to the tensor terms of SAMi-T. In order to explore mode details of the effects of tensor force, we perform the calculations with or without tensor terms using SAMi-T EDF. Figure 3 shows the β -decay half-lives calculated by RPA and SSRPA with SAMi-T including or excluding tensor terms. In the figure, the results calculated with SAMi-T with and without tensor terms are labeled by “w/i-T” and “w/o-T,” respectively. The tensor force will reduce the half-lives in ^{34}Si and ^{78}Ni greatly on the RPA level, but the results are still larger than the experimental values. Moreover, the lifetimes of ^{68}Ni and ^{132}Sn are infinite in RPA calculations even with the tensor terms. Similar to the results obtained by SAMi shown in Fig. 2, the SSRPA calculation with SAMi-T excluding tensor force reduces the half-lives in ^{34}Si and ^{78}Ni by more than two orders of magnitude compared with the RPA results. However, these results still overestimate the half-lives of ^{68}Ni and ^{132}Sn . With the tensor force in SSRPA calculations, the half-lives of ^{132}Sn and ^{68}Ni are reduced by a factor larger than 5, while the half-life of ^{34}Si is enhanced about 30 times. Consequently, the half-lives of ^{132}Sn , ^{78}Ni , and ^{34}Si are reproduced with high accuracy by the SSRPA with the tensor, though the half-life of ^{68}Ni

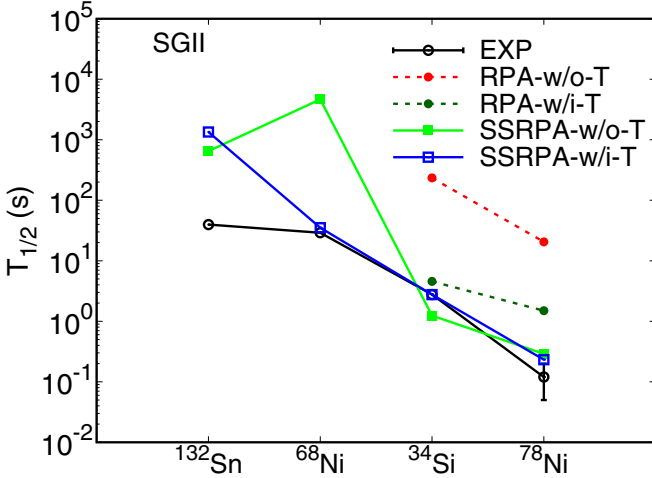


FIG. 4. The same as Fig. 3 but for DEF SGII. The red and dark green solid circles represent RPA results with SGII excluding and including tensor terms $T(500, -280)$, respectively. The green filled squares represent SSRPA results with SGII without tensor terms. The blue empty squares represent SSRPA results with SGII including tensor terms $T(500, -280)$. The experimental data are shown by the black empty circles.

is still overestimated. In Ref. [62], the strengths of tensor terms were constrained with the main peak energies of GT and charge-exchange spin-dipole transitions based on RPA calculations. However, the parameters have still some freedom to be adjusted with new constraints. In Ref. [50], we checked by SSRPA that SGII+ $Te1$ is able to produce more realistic results than other EDFs for the GT giant resonances. In the present work, in order to find a better choice of strengths of

tensor terms, we did various calculations changing parameters of the tensor force around the parameter set SGII+ $Te1$, and found that SGII+ $T(500, -280)$ is the best to give realistic descriptions for both quantities. It should be noticed that the strengths of tensor terms are different from SAMi-T with $(T, U) = (415.5, -95.5)$. The triplet-even term is close to SGII+ $T(500, -280)$, but the triplet-odd term is weaker by about a factor of 3. Figure 4 shows the β -decay half-lives of ^{132}Sn , ^{68}Ni , ^{34}Si , and ^{78}Ni calculated by RPA and SSRPA with and without SGII including tensor terms $T(500, -280)$. The effects of tensor force in RPA calculations are similar to those in SAMi-T EDF. The tensor force reduces the half-lives in ^{34}Si and ^{78}Ni greatly on the RPA level, but cannot produce finite lifetimes in ^{68}Ni and ^{132}Sn . The effects of including 2p-2h configurations in SSRPA are clear in this figure, which reduce the β -decay half-lives in ^{78}Ni and ^{34}Si by two orders of magnitude, and give finite half-lives for ^{132}Sn and ^{68}Ni . The effect of tensor force in SSRPA calculation is observed mainly in ^{68}Ni , where the tensor force reduces the half-life by two order of magnitude, while in ^{34}Si the tensor terms enhance slightly the half-life.

In order to see more detail about how the 2p-2h correlations and tensor force affect the β decay, the GT strength distributions are shown in Fig. 5 calculated by RPA with SGII, and SSRPA with SGII and SGII+ $T(500, -280)$ EDFs, in which the excitation energies are referred to the ground states of daughter nuclei. In RPA calculations, for ^{132}Sn and ^{68}Ni [Figs. 5(a) and 5(b)], the lowest GT states are above the Q_β windows, not seeing the view graphs, which lead to the infinite half-lives. For ^{34}Si shown in Fig. 5(c), the RPA calculation gives a low-energy GT state, but the strength is much smaller. Furthermore, for ^{78}Ni shown in Fig. 5(d), the RPA states have the excitation energies slightly lower than the β -decay window. Consequently, the half-lives of the two nuclei

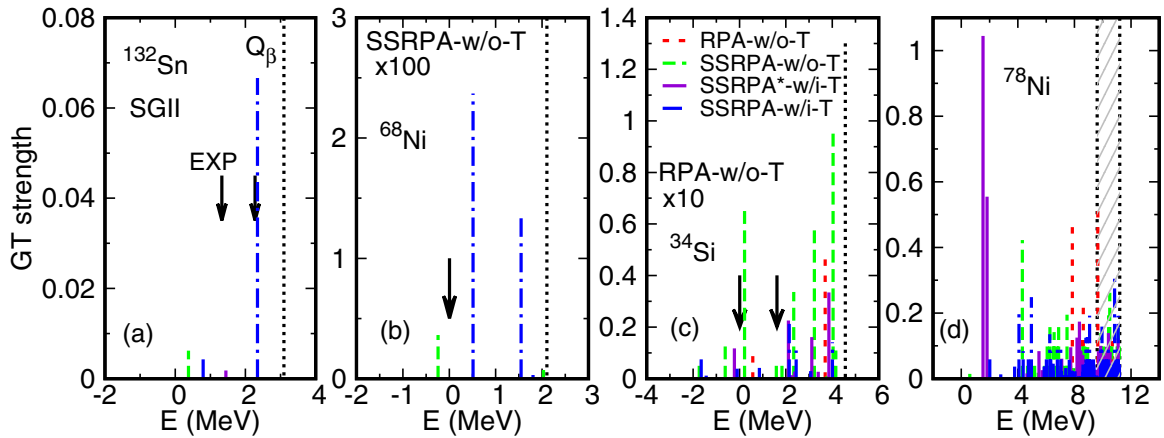


FIG. 5. The GT strength distributions with respect to the daughter nucleus in ^{132}Sn , ^{68}Ni , ^{34}Si , and ^{78}Ni calculated by RPA with SGII and SSRPA with SGII and SGII+ $T(500, -280)$. The observed excitation energies of GT states are marked by the arrows [13]. The red dashed lines and the green dashed lines represent results obtained with SGII by RPA and SSRPA, labeled “RPA-w/o-T” and “SSRPA-w/o-T” respectively. The dark violet lines represent the results obtained by SSRPA with SGII+ $T(500, -280)$ in which tensor terms are included only in HF calculations, labeled “SSRPA*-w/i-T.” The blue dash-dotted lines represent the results obtained by SSRPA with SGII+ $T(500, -280)$ in which tensor terms are included both in HF and SSRPA calculations, labeled “SSRPA-w/i-T.” The positions higher than the energy of β decay are neglected and the experimental energies of β -decay Q values are shown by the black dotted lines and the gray zone in ^{78}Ni due to a large experimental uncertainty. To facilitate the comparison of different strengths, the strengths in the figure have been multiplied a factor which appears in each window.

in the RPA model are much longer than the experimental values.

The effects of tensor force at the mean-field level and the dynamic effects in RPA are discussed in details in Ref. [63]. In SSRPA calculations, the comparison between the effects of tensor force at the mean-field level and the dynamic effects are exhibited in Fig. 5 by different colored lines. The GT strength distributions of ^{132}Sn , ^{68}Ni , and ^{34}Si are moved to a higher energy region if the tensor terms are included only in HF calculations (dark violet), but the GT strength distributions are moved to a lower energy region when the tensor terms are included in both HF and SSRPA calculations (blue). In ^{78}Ni , these two effects are reversed; the tensor terms in HF lower the GT strength since the single-particle energy of neutron $1g_{9/2}$ orbit is lowered by the tensor correlation, while the SSRPA with tensor terms pushes up the GT strength in energy. It seems that the roles of the two effects depend on the shell structure of each nucleus. This point should be studied further in future work.

In both self-consistent SSRPA calculations with and without tensor force for the four nuclei (green and blue results), the obtained GT states are distributed in sufficiently low-energy regions close to the experimental data, which lead to finite reasonable half-lives in comparison with the experimental values. However, in ^{132}Sn and ^{68}Ni , the strengths calculated without tensor force are small below the Q_β windows, which produce much longer half-lives. In SSRPA calculations with tensor force, the strengths are strong enough in $^{68,78}\text{Ni}$ and ^{34}Si , and hence half-lives become close to the experimental ones. However, in ^{132}Sn , the calculated GT strength in the low-energy region is small and the half-life is still much longer.

IV. SUMMARY

In summary, we studied the half-lives of β decay in four magic and semimagic nuclei ^{132}Sn , ^{68}Ni , ^{34}Si , and ^{78}Ni , using the self-consistent HF+SSRPA model with different Skyrme EDFs. In the present work, we focus on the EDFs SGII, SAMi, SAMi-T, which are better at describing the giant GT resonances in four closed-shell nuclei including ^{132}Sn [50]. We adopted the strength of triplet-even and triplet-odd tensor terms $(T, U) = (500, -280)$ in SGII+ $T(500, -280)$, which are close to the values adopted in SGII+ $Te1$ EDF. In RPA calculations, the calculated half-lives are much longer than experiments and become infinite in ^{132}Sn and ^{68}Ni . Compared with the RPA model, the inclusion of 2p-2h configurations in

the SSRPA model in general can reduce systematically the lifetimes of β decay in the four nuclei. In particular, it accelerates the β -decay rates of ^{34}Si and ^{78}Ni by about two order of magnitude and also produces finite half-lives for long-living nuclei ^{132}Sn and ^{68}Ni .

The effects of the tensor force in SSRPA are studied with the two EDFs, SAMi-T and SGII+ $T(500, -280)$. In SAMi-T, the tensor force accelerates the β -decay rates of ^{132}Sn and ^{68}Ni by about five times, while it increases the half-life of ^{34}Si significantly. In the case of SGII+ $T(500, -280)$, the effect of tensor force is mainly observed in ^{68}Ni , in which the decay rate is accelerated by about two order of magnitude.

To see more details of the effects of 2p-2h configurations and the tensor force, the low-lying GT states are calculated with SGII and SGII+ $T(500, -280)$. In ^{34}Si and ^{78}Ni , the 2p-2h correlations shift enough strength to the low-energy region below the β -decay Q value and produce half-lives very close to the experimental ones, but in ^{132}Sn and ^{68}Ni the GT strengths are too small to reproduce the experimental half-lives. On top of the 2p-2h effect, the tensor force shifts substantial strength in ^{68}Ni to the low-energy region and reproduces the experimental half-life. However, in ^{132}Sn , the tensor force in SGII+ $T(500, -280)$ cannot shift enough strength to the low-energy region, and the half-life is still overestimated.

The EDFs adopted in the present study cannot reproduce systematically the experimental half-lives for all nuclei, as well as the GT resonances simultaneously. As far as the β -decay half-life is concerned, SSRPA calculations with SLy5 and SKM* can reproduce the experimental data well, but they are poor at describing the giant GT and spin-dipole resonances. For the consistent descriptions of the β -decay half-life as well as other spin-isospin observables such as the giant GT resonance, we should study further optimal EDFs with tensor terms in the beyond-mean-field framework such as SSRPA.

ACKNOWLEDGMENTS

We are grateful to Profs. M. Grasso and D. Gambacurta for fruitful discussions. This work is supported by the National Natural Science Foundation of China under Grants No. 11575120 and No. 11822504, by the Science Specialty Program of Sichuan University under Grants No. 2020SCUNL209 and No. 2020SCUNL210, and by The JSPS Grant-in-Aid for Scientific Research (C) under Grant No. 19K03858.

-
- [1] K. Grotz and H. V. Klapdor, *The Weak Interaction in Nuclear, Particle, and Astrophysics*, (Adam Hilger, Bristol, UK, 1990).
 - [2] K. Langanke and G. Martínez-Pinedo, *Rev. Mod. Phys.* **75**, 819 (2003).
 - [3] E. M. Burbidge, G. R. Burbidge, W. A. Fowler, and F. Hoyle, *Rev. Mod. Phys.* **29**, 547 (1957).
 - [4] I. N. Borzov, *Nucl. Phys. A* **777**, 645 (2006).
 - [5] Y.-Z. Qian and G. Wasserburg, *Phys. Rep.* **442**, 237 (2007).
 - [6] M. Arnould, S. Goriely, and K. Takahashi, *Phys. Rep.* **450**, 97 (2007).
 - [7] J. J. Cowan, F.-K. Thielemann, and J. W. Truran, *Phys. Rep.* **208**, 267 (1991).
 - [8] S. Nishimura, Z. Li, H. Watanabe, K. Yoshinaga, T. Sumikama, T. Tachibana, K. Yamaguchi, M. Kurata-Nishimura, G. Lorusso, Y. Miyashita, A. Odahara, H. Baba, J. S. Berryman, N. Blasi, A. Bracco, F. Camera, J. Chiba, P. Doornenbal, S. Go, T. Hashimoto *et al.*, *Phys. Rev. Lett.* **106**, 052502 (2011).

- [9] G. Lorusso, S. Nishimura, Z. Y. Xu, A. Jungclaus, Y. Shimizu, G. S. Simpson, P.-A. Söderström, H. Watanabe, F. Browne, P. Doornenbal, G. Gey, H. S. Jung, B. Meyer, T. Sumikama, J. Taprogge, Z. Vajta, J. Wu, H. Baba, G. Benzoni, K. Y. Chae *et al.*, *Phys. Rev. Lett.* **114**, 192501 (2015).
- [10] J. Wu, S. Nishimura, G. Lorusso, P. Möller, E. Ideguchi, P.-H. Regan, G. S. Simpson, P.-A. Söderström, P. M. Walker, H. Watanabe, Z. Y. Xu, H. Baba, F. Browne, R. Daido, P. Doornenbal, Y. F. Fang, N. Fukuda, G. Gey, T. Isobe, Z. Korkulu *et al.*, *Phys. Rev. Lett.* **118**, 072701 (2017).
- [11] G. Audi, F. G. Kondev, M. Wang, W. J. Huang, and S. Naimi, *Chin. Phys. C* **41**, 030001 (2017).
- [12] M. Wang, G. Audi, F. G. Kondev, W. J. Huang, S. Naimi, and X. Xu, *Chin. Phys. C* **41**, 030003 (2017).
- [13] <http://www.nndc.bnl.gov>
- [14] K. Takahashi and M. Yamada, *Prog. Theor. Phys.* **41**, 1470 (1969).
- [15] K. Takahashi, M. Yamada, and T. Kondoh, *At. Data Nucl. Data Tables* **12**, 101 (1973).
- [16] T. Tachibana, M. Yamada, and Y. Yoshida, *Prog. Theor. Phys.* **84**, 641 (1990).
- [17] E. Caurier, G. Martínez-Pinedo, F. Nowack, A. Poves, and A. P. Zuker, *Rev. Mod. Phys.* **77**, 427 (2005).
- [18] B. R. Barrett, P. Navrátil, and J. P. Vary, *Prog. Part. Nucl. Phys.* **69**, 131 (2013).
- [19] J. Kruminde and P. Möller, *Nucl. Phys. A* **417**, 419 (1984).
- [20] P. Möller and J. Randrup, *Nucl. Phys. A* **514**, 1 (1990).
- [21] K. Langanke and G. Martínez-Pinedo, *Nucl. Phys. A* **673**, 481 (2000).
- [22] G. Martínez-Pinedo and K. Langanke, *Phys. Rev. Lett.* **83**, 4502 (1999).
- [23] J. J. Cuenca-García, G. Martínez-Pinedo, K. Langanke, F. Nowacki, and I. N. Borzov, *Eur. Phys. J. A* **34**, 99 (2007).
- [24] T. Suzuki, T. Yoshida, T. Kajino, and T. Otsuka, *Phys. Rev. C* **85**, 015802 (2012).
- [25] Q. Zhi, E. Caurier, J. J. Cuenca-García, K. Langanke, G. Martínez-Pinedo, and K. Sieja, *Phys. Rev. C* **87**, 025803 (2013).
- [26] H. T. Li and Z. Z. Ren, *J. Phys. G* **41**, 105102 (2014).
- [27] V. Kumar, P. C. Srivastava, and H. T. Li, *J. Phys. G* **43**, 105104 (2016).
- [28] S. Yoshida, Y. Utsuno, N. Shimizu, and T. Otsuka, *Phys. Rev. C* **97**, 054321 (2018).
- [29] J. Engel, M. Bender, J. Dobaczewski, W. Nazarewicz, and R. Surman, *Phys. Rev. C* **60**, 014302 (1999).
- [30] T. Nikšić, T. Marketin, D. Vretenar, N. Paar, and P. Ring, *Phys. Rev. C* **71**, 014308 (2005).
- [31] T. Marketin, D. Vretenar, and P. Ring, *Phys. Rev. C* **75**, 024304 (2007).
- [32] D. L. Fang, B. A. Brown, and T. Suzuki, *Phys. Rev. C* **88**, 024314 (2013).
- [33] Z. M. Niu, Y. F. Niu, H. Z. Liang, W. H. Long, T. Nikšić, D. Vretenar, and J. Meng, *Phys. Lett. B* **723**, 172 (2013).
- [34] D. Ni and Z. Ren, *Phys. Rev. C* **89**, 064320 (2014).
- [35] M. T. Mustonen and J. Engel, *Phys. Rev. C* **93**, 014304 (2016).
- [36] T. Marketin, L. Huther, and G. Martínez-Pinedo, *Phys. Rev. C* **93**, 025805 (2016).
- [37] D. L. Fang, *Phys. Rev. C* **93**, 034306 (2016).
- [38] F. Minato and C. L. Bai, *Phys. Rev. Lett.* **110**, 122501 (2013).
- [39] D. Z. Chen, D. L. Fang, and C. L. Bai, *Nucl. Sci. Tech.* **32**, 74 (2021).
- [40] B. Dai, B. S. Hu, Y. Z. Ma, J. G. Li, S. M. Wang, C. W. Johnson, and F. R. Xu, *Phys. Rev. C* **103**, 064327 (2021).
- [41] C. L. Bai, D. L. Fang, and H. Q. Zhang, *Chin. Phys. C* **46**, 114104 (2022).
- [42] J. Speth and A. van der Woude, *Rep. Prog. Phys.* **44**, 719 (1981).
- [43] A. Van Der Woude, *Prog. Part. Nucl. Phys.* **18**, 217 (1987).
- [44] A. P. Severyukhin, V. V. Voronov, I. N. Borzov, N. N. Arsenyev, and N. Van Giai, *Phys. Rev. C* **90**, 044320 (2014).
- [45] Y. F. Niu, Z. M. Niu, G. Colò, and E. Vigezzi, *Phys. Rev. Lett.* **114**, 142501 (2015).
- [46] Y. F. Niu, G. Colò, E. Vigezzi, C. L. Bai, and H. Sagawa, *Phys. Rev. C* **94**, 064328 (2016).
- [47] Y. F. Niu, Z. M. Niu, G. Colò, and E. Vigezzi, *Phys. Lett. B* **780**, 325 (2018).
- [48] D. Gambacurta, M. Grasso, and J. Engel, *Phys. Rev. Lett.* **125**, 212501 (2020).
- [49] D. Gambacurta and M. Grasso, *Phys. Rev. C* **105**, 014321 (2022).
- [50] M. J. Yang, C. L. Bai, H. Sagawa, and H. Q. Zhang, *Phys. Rev. C* **106**, 014319 (2022).
- [51] S. Ait-Tahar and D. Brink, *Nucl. Phys. A* **560**, 765 (1993).
- [52] D. Gambacurta, M. Grasso, and F. Catara, *Phys. Rev. C* **81**, 054312 (2010).
- [53] D. Gambacurta, M. Grasso, and J. Engel, *Phys. Rev. C* **92**, 034303 (2015).
- [54] M. J. Yang, C. L. Bai, H. Sagawa, and H. Q. Zhang, *Phys. Rev. C* **103**, 054308 (2021).
- [55] I. N. Borzov and S. Goriely, *Phys. Rev. C* **62**, 035501 (2000).
- [56] J. Bartel, P. Quentin, M. Brack, C. Guet, and H.-B. Hokansson, *Nucl. Phys. A* **386**, 79 (1982).
- [57] M. Beiner, H. Flocard, N. Van Giai, and P. Quentin, *Nucl. Phys. A* **238**, 29 (1975).
- [58] E. Chabanat, P. Bonche, P. Haensel, J. Meyer, and R. Schaeffer, *Nucl. Phys. A* **635**, 231 (1998).
- [59] N. Van Giai and H. Sagawa, *Phys. Lett. B* **106**, 379 (1981).
- [60] X. Roca-Maza, G. Colò, and H. Sagawa, *Phys. Rev. C* **86**, 031306(R) (2012).
- [61] S. H. Shen, G. Colò, and X. Roca-Maza, *Phys. Rev. C* **99**, 034322 (2019).
- [62] C. L. Bai, H. Q. Zhang, H. Sagawa, X. Z. Zhang, G. Colò, and F. R. Xu, *Phys. Rev. C* **83**, 054316 (2011).
- [63] C. L. Bai, H. Sagawa, H. Q. Zhang, X. Z. Zhang, G. Colò, and F. R. Xu, *Phys. Lett. B* **675**, 28 (2009).